IOPscience iopscience.iop.org

Home Search Collections Journals About Contact us My IOPscience

Effects of deposition parameters on microstructure of CrN/Si_3N_4 nanolayered coatings and their thermal stability

This article has been downloaded from IOPscience. Please scroll down to see the full text article.

2005 J. Phys.: Condens. Matter 17 6405

(http://iopscience.iop.org/0953-8984/17/41/011)

View the table of contents for this issue, or go to the journal homepage for more

Download details:
IP Address: 129.252.86.83
The article was downloaded on 28/05/2010 at 06:10

Please note that terms and conditions apply.

INSTITUTE OF PHYSICS PUBLISHING JOURNAL OF PHYSICS: CONDENSED MATTER

J. Phys.: Condens. Matter **17** (2005) 6405–6413 doi:10.1088/0953-8984/17/41/011

Effects of deposition parameters on microstructure of CrN/Si_3N_4 nanolayered coatings and their thermal stability

Xiaoming Bai, Weitao Zheng[1], Tao An and Qing Jiang

Department of Materials Science, Key Laboratory of Automobile Materials of MOE, and State Key Laboratory of Superhard Materials, Jilin University, Changchun 130012, People's Republic of China

E-mail: WTZheng@jlu.edu.cn

Received 15 July 2005, in final form 15 September 2005
Published 30 September 2005
Online at stacks.iop.org/JPhysCM/17/6405

Abstract

Polycrystalline CrN/Si_3N_4 multilayer films were deposited by using two reactive magnetron sputtering targets, Cr and Si, respectively, and the as-deposited multilayer coatings were annealed at 900 °C for 2–4 h in vacuum. We investigated the effects of mixed discharge gas pressure, bias voltage, substrate temperature and annealing temperature on the microstructural and interfacial properties of polycrystalline CrN/Si_3N_4 multilayer films. X-ray diffraction and x-ray reflectivity measurements showed that the layer structure of the coatings is maintained even after annealing at 900 °C for 4 h when the Si_3N_4 layer thickness is 0.3 nm, which meant that with proper control of the Si_3N_4 thickness CrN/Si_3N_4 multilayer coatings had an excellent thermal stability and were potential candidates for high-temperature tribological applications.

(Some figures in this article are in colour only in the electronic version)

1. Introduction

There has been increasing interest in protective coatings for cutting tools under dry machining conditions [1]. This is mainly due to environmental and economic concerns about the use of coolants/lubricants in the machining process. Nanolayered coatings can play an important role in this area, as they can provide high hardness and a low friction coefficient at room temperature. However, machining at high speeds without coolants can easily raise tool temperatures to 800–1000 °C. In many cases, nanolayered coatings are unstable due to inter-diffusion or other degradation at elevated temperatures, leading to a decrease in hardness and coating

[1] Author to whom any correspondence should be addressed.

© 2005 IOP Publishing Ltd Printed in the UK

degradation. The key to minimizing such instability is to use immiscible components with low energy interfaces in nanolayered coatings.

In the past decades, TiN-based films deposited by the physical vapour deposition (PVD) or chemical vapour deposition (CVD) method have found widespread applications in wear resistant situations such as cutting tools or machine parts because of their high hardness, wear resistance, chemical inertness, and high temperature stability. Veprek [2–6] reported superhard Ti–Si–N nanocomposite films with a hardness of 80–105 GPa, which is higher than that of diamond (70–90 GPa), and he has proposed a two-phase structure model to interpret the superhardness mechanism of nanocomposite films. According to the model, because Si_3N_4 is immiscible with TiN and can wet the growing surface of TiN grains, Ti–Si–N nanocomposite films form a structure of nanocrystalline (nc) TiN surrounded by amorphous Si_3N_4, known as nc-TiN/a-Si_3N_4. This concept is based on a strong, thermodynamically driven, and diffusion-rate-controlled (spinodal) phase segregation that leads to the formation of a stable nanostructure by self-organization.

Me–Si–N nanocomposite films (Me represents transition metals, such as Ti, V, and W) show the superhardness effect too. Recently, an increasing amount of attention has been focused on other metal nitrides grown by PVD processes, such as CrN, VN [7], ZrN [8] and W_2N [3], with specific interest in Cr–N and Si_3N_4. It was found that CrN [9] coatings exhibit excellent corrosion and wear properties, and have better oxidation resistance, as well as better adhesion to tool steel when compared to TiN films. Xu [10] reported that the superhardness effect was not observed in the CrN/Si_3N_4 nano-structured multilayer films on Si(100) wafers fabricated by radio-frequency reactive magnetron sputtering. Martinez [11] investigated the nanocomposite Cr–Si–N films deposited by reactive magnetron sputtering at 510 K using two confocal targets of Cr and Si. A maximum hardness value (26 GPa) has been found for a structure composed of 4 nm CrN crystallites embedded in amorphous Si_3N_4. So far no results have been reported [12] about the thermal stability and diffusion behaviour of the PVD CrN/Si_3N_4 nano-structured multilayers.

It is difficult to directly observe the structure of the Si_3N_4 interfacial phase in superhard nanocomposite films using a high-resolution transmission electron microscope (HRTEM) because its thickness is usually less than 1 nm [13]. Although the researchers have considered the interfacial phase as an amorphous solid, there are no direct experimental results, such as HRTEM images, to reveal the structure in superhard nanocomposite films with low Si content. For two-dimensional multilayers, it is easy to control the thickness of the modulation layers. Therefore, in this work, the focus of our study is CrN/Si_3N_4 nanolayered coatings. A series of CrN/Si_3N_4 multilayers with different thickness of Si_3N_4 layers are deposited to simulate the interface of Cr–Si–N nanocomposite films. The influence of the thickness of Si_3N_4 layers and other deposition parameters such as pressure, bias and temperature on the interfacial structure and microstructure of the multilayers is studied. The thermal stability of the multilayers is also investigated by means of annealing at 900 °C for 2–4 h in vacuum.

2. Experimental procedures

CrN/Si_3N_4 multilayers were deposited using a JGP450A magnetron sputtering system, which has four independent cathodes (three dc and one rf cathodes). Cr (99.99%) and Si (99.99%) were used as targets, placed on the dc and rf cathodes respectively. The substrate material was an Si(100) wafer with dimensions of $25 \times 25 \times 0.7$ mm^3. Prior to the coating process, the Si wafers were ultrasonically cleaned in acetone and alcohol and then mounted on the rotatable substrate holder. Before deposition, the chamber was preheated and evacuated to 1.4×10^{-4} Pa to avoid contamination during the deposition process, and then high-purity working gas and

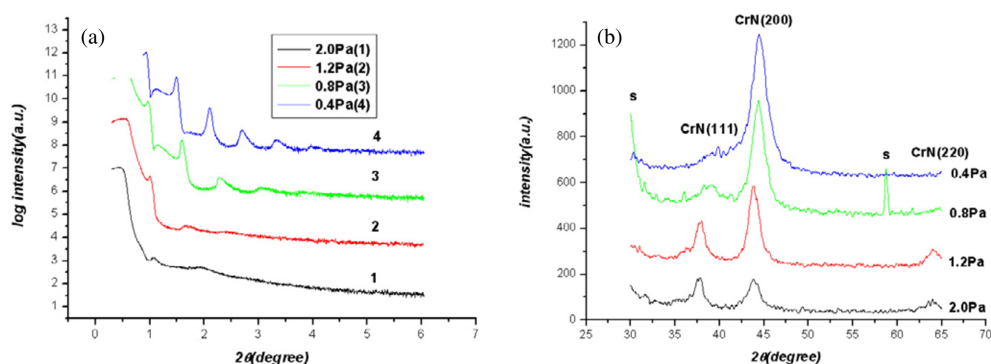

Figure 1. (a) XRR and (b) XRD spectra of CrN/Si_3N_4 multilayer deposited at different deposition pressures (substrate retention time for Cr target, 33 s; Si, 32 s; 40 layers).

reactive gas were introduced, using mass flow controllers to regulate both gas flows. Argon (99.999%) gas flow rate was fixed at 30.0 sccm. Nitrogen gas (99.999%) flow rate was fixed at 10.0 sccm. The power of Cr and Si targets was 54 W ($I = 0.2$ A, $U = 270$ V) and 200 W ($I = 0.275$ A, $U = 800$ V, $P_r = 10$ W), respectively. The working pressure was fixed at certain values by regulation of the vacuum valve. Under these deposition conditions, a series of multilayers with 40 layers was obtained through the control of the bias, pressure, temperature and retention time (Cr, 33 s; Si, 32 s) in front of Cr and Si targets. For the comparison of layer structure and diffusion behaviour with CrN/Si_3N_4 multilayers, a series of TiN/Si_3N_4 multilayers with 20 layers were also deposited under −140 V, 0.8 Pa (Ti target power 104 W, $I = 0.4$ A, $U = 260$ V).

The multilayer structure of the films was determined by x-ray reflectivity (XRR) using a D8tools diffractor with Cu Kα radiation ($U = 40$ kV, $I = 40$ mA, scan step 0.004°, scan speed 0.5 s/step). The microstructure of the films was determined by x-ray diffraction (XRD) using a diffractometer (Rigaku) with Cu Kα radiation ($P = 12.5$ kW, scan step 0.02°). A Digital Instruments Nanoscope III atomic force microscope (AFM) was used in tapping mode with a scan frequency of 1.0 Hz to measure the surface structure and roughness of the films.

To assess the thermal stability of CrN/Si_3N_4 multilayer coatings, we used a vacuum furnace capable of reaching 1000 °C. The vacuum chamber was first pumped down to 1.4×10^{-4} Pa. The temperature was increased to 900 °C at a rate of 10 °C min^{-1}. This final temperature was maintained for 2 or 4 h. The temperature was also decreased at a rate of 10 °C min^{-1} after annealing.

3. Results and discussion

3.1. The effect of deposition parameters

3.1.1. Deposition pressure. Four samples deposited at different deposition pressures without bias were prepared. Figures 1(a) and (b) show their XRR and XRD spectra. The XRR spectra indicate that the layer structure becomes more apparent as the deposition pressure decreases, which is probably due to the increasing energy of ions discharged coming into the growing film, leading to improving the interfacial roughness. The energetic sputtered ions play an important role in the film growth mechanisms. The increasing gas pressure may cause an increasing number of collisions between CrN, Si_3N_4 and gas particles. The CrN and Si_3N_4

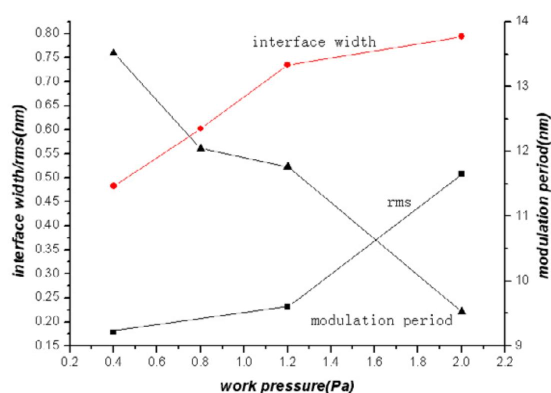

Figure 2. The relation between modulation period Λ (interface width, rms) and pressure of a mixture of Ar and N_2, in which the lines are just guides to the eyes.

particles sputtered from target undergo collision with the discharge gas, losing their energy in this process. The particles do not have enough energy to diffuse on the surface of the growing films and to fill the microholes and pores, leading to poor interfacial smoothness.

The collision effect also affects the deposition rate and multilayer period. The modulation period can be determined by the position of the main Bragg peaks [14]

$$m\lambda = 2\Lambda[\sin\theta_m - (1-\delta)/\sin\theta_m] \qquad (1)$$

where λ represents the x-ray wavelength; θ_m is the Bragg angle corresponding to the mth order reflection. The interface sharpness can be estimated by $\Lambda/4(n_{\max}+1)$ [15], where Λ is the modulation period; $n_{\max}$ is the highest order of the observed low angle peaks. Figure 2 shows the effects of deposition pressure of a mixture of Ar and N_2 on modulation period Λ, interface width and rms. The XRR results show that with the increase of pressure the modulation periods of the multilayer decrease, but the interface widths and the mean roughness increase.

XRD patterns of CrN/Si_3N_4 multilayer coatings deposited at different pressures are shown in figure 1(b). All multilayer coatings show CrN (111), (200) and (220) preferred orientation. The (111) and (220) peak intensity decreases and the (200) peak intensity increases as the deposition pressure decreases from 2.0 to 0.4 Pa, which is due to more intense ion bombardment. As deposition pressure increases, the shifting of the peak position to lower angles is related to the change of internal stress generated by ion bombardment [16].

3.1.2. Substrate bias. Four samples deposited at different substrate biases at deposition pressure 0.8 Pa were prepared. Figures 3(a) and (b) show their XRR and XRD spectra. The XRR spectra indicate that the layer structure is not apparent at floating voltage. As the substrate bias increases, the layer structure becomes more apparent (12th and 11th order reflection peaks appear). As the substrate bias increases further, the layer structure becomes not more apparent (only tenth and ninth order reflection peaks appear). This is probably due to the increase of energy coming into the growing film and improvement of the interfacial smoothness [17]. Higher substrate bias results in strong ion bombardment, leading to excessive layer intermixing or ion implanting, whereas lower substrate bias or floating voltage does not provide sufficient mobility to surface species during deposition, resulting in rough interfaces.

XRD patterns of CrN/Si_3N_4 multilayer coatings deposited at different substrate biases and deposition pressure 0.8 Pa shown in figure 3(b). The multilayer coating at floating voltage shows CrN(111) and (200) preferred orientation and those at other different substrate biases

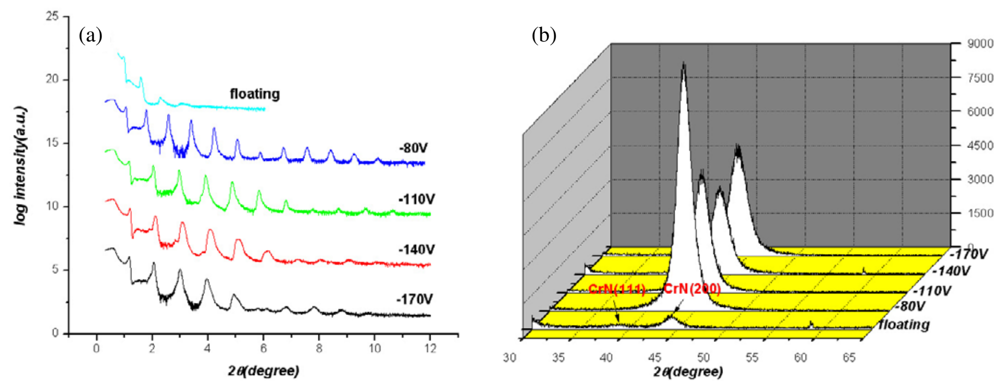

Figure 3. (a) XRR and (b) XRD spectra of CrN/Si_3N_4 multilayer with different substrate biases at deposition pressure 0.8 Pa (substrate retention time for Cr target, 33 s; Si, 32 s; 40 layers).

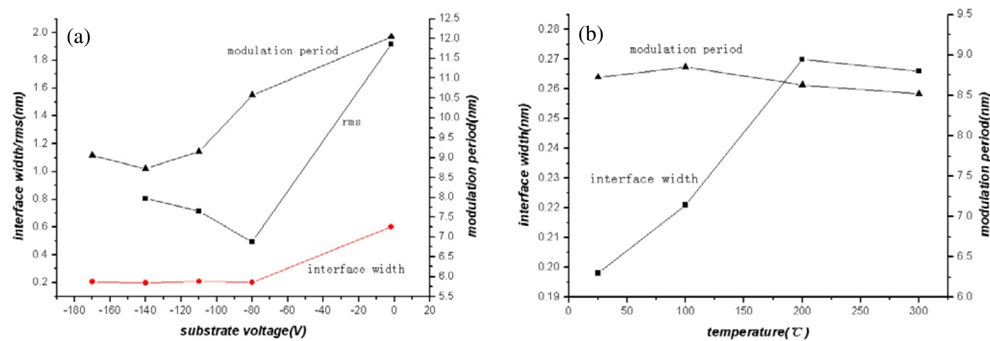

Figure 4. (a) The relation between modulation period Λ (interface width, rms) and bias voltage. (b) The relation between modulation period Λ (interface width) and substrate temperature.

show only CrN(111) preferred orientation. The (200) peak intensity is strong at bias −80 V and becomes less strong at other biases. The substrate bias plays an important role in the microstructure of CrN/Si_3N_4 multilayer.

Figure 4(a) shows that with the increase of absolute bias voltage the modulation periods of the multilayer increase but mean roughness decreases first, and then increases, and has a minimum value of 0.495 nm at −80 V. The interface widths decrease first and then remain almost unchanged.

3.1.3. Substrate temperature. Three samples deposited at different substrate temperatures with a bias voltage of −140 V and deposition pressure 0.8 Pa were prepared. Figures 5(a) and (b) show their XRR and XRD spectra. The XRR spectra indicate that the layer structure is apparent at room temperature (tenth order reflection peaks appear). As the substrate temperature increases, the layer structure becomes less apparent (only ninth and seventh order reflection peaks appear), which is probably due to the increasing of layer intermixing and interfacial roughness. The XRD spectra reveal that the (200) peak intensity decreases as the substrate temperature increases. At 300 °C, the (200) peak becomes very weak and a weak (111) peak appears.

Figure 4(b) shows the effects of substrate temperature on the modulation period Λ and interface width. As the substrate temperature increases, the modulation period Λ remains

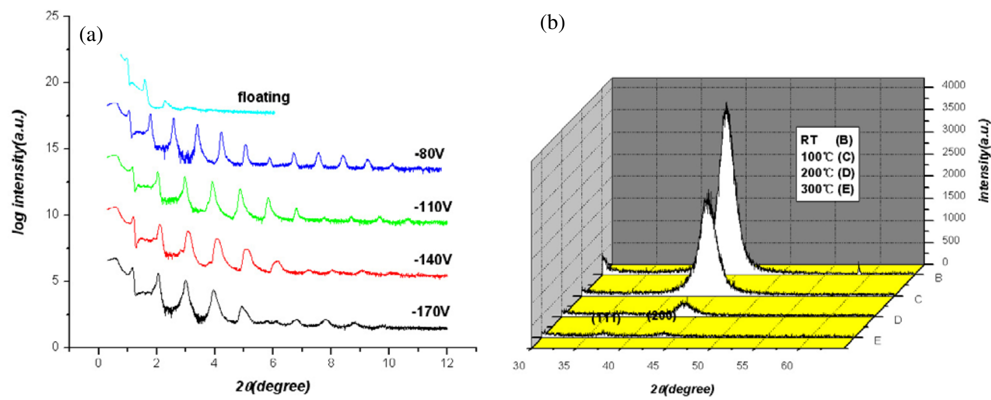

Figure 5. (a) XRR and (b) XRD spectra of CrN/Si_3N_4 multilayer with different substrate temperatures at bias of −140 V voltage and deposition pressure 0.8 Pa (substrate retention time for Cr target, 33 s; Si, 32 s; 40 layers).

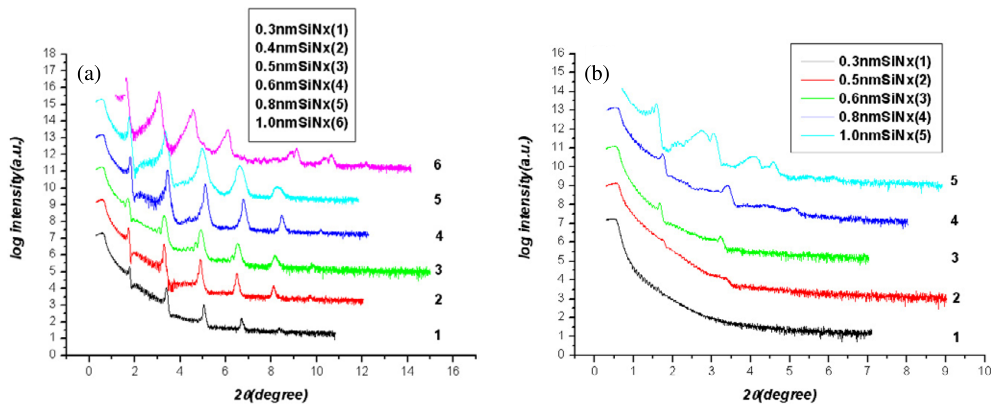

Figure 6. (a) As-deposited CrN/Si_3N_4 multilayers with different Si_3N_4 layer thicknesses (CrN layer thickness 5.0 nm, 20 layers). (b) As-deposited TiN/Si_3N_4 multilayers with different Si_3N_4 layer thickness (TiN layer thickness 5.0 nm, 20 layers).

almost unchanged but the interface width increases due to the enhancement of inter-diffusion at higher substrate temperature.

3.2. The thermal stability

3.2.1. The layer intermixing of as-deposited multilayers with different Si_3N_4 layer thicknesses. A series of samples which the CrN layer thickness is maintained at 5 nm and Si_3N_4 layer thickness varies from 1 to 0.3 nm were prepared at bias of −140 V, pressure of 0.8 Pa, and room temperature. Figure 6(a) shows their XRR spectra. We can see that the multilayer has apparent periodic layer structure even when Si_3N_4 layer thickness decreases to 0.3 nm. It may cause the interfaces to be very sharp that the CrN and Si_3N_4 are immiscible and do not form an interfacial phase. To compare the diffusion behaviour of Si_3N_4 in transition metal nitride, we also prepared a series of TiN/Si_3N_4 samples [18] in which the TiN layer thickness is maintained at 5 nm and Si_3N_4 layer thickness varies from 1 to 0.3 nm. From their XRR spectra shown in figure 6(b) we can see that the layer structure of the coating disappeared

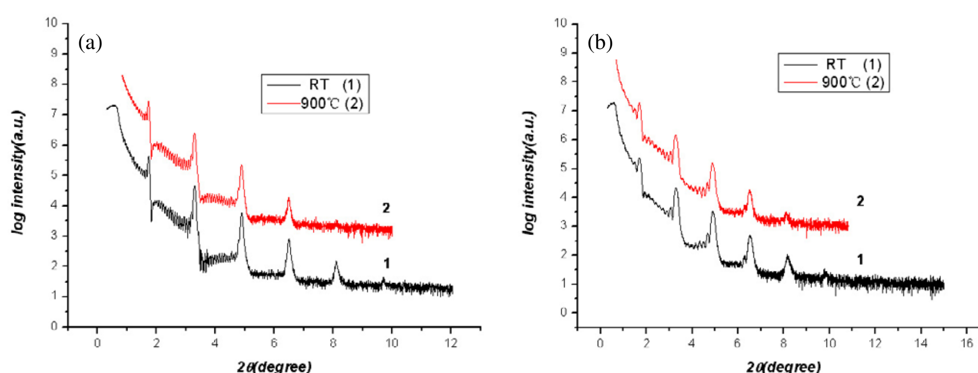

Figure 7. XRR patterns of CrN/Si_3N_4 coatings (20 layers) deposited at room temperature and after annealing at 900 °C for 2 h in which (a) CrN/Si_3N_4 layer thickness is 5.0/0.4 nm; (b) CrN/Si_3N_4 layer thickness is 5.0/0.5 nm.

when the Si_3N_4 layer thickness was 0.3 nm, and the number of XRR diffraction peaks for other samples was obviously less than that for CrN/Si_3N_4 samples. This means that Si_3N_4 diffuses with more difficulty in CrN than in TiN. According to Veprek, the superhardness of nanocomposite coatings is based on a strong, thermodynamically driven, and diffusion-rate-controlled (spinodal) phase segregation that leads to the formation of a stable nanostructure by self-organization [19]. The poor diffusion rate of Si_3N_4 in CrN probably confines the formation of nano-crystalline CrN surrounded perfectly by one monolayer Si_3N_4 and so causes poor hardness.

3.2.2. Thermal stability. Figures 7(a) and (b) are XRR patterns of CrN/Si_3N_4 coatings deposited at room temperature and after annealing at 900 °C for 2 h at various thickness values of the S_3N_4 layer. When the S_3N_4 layer thickness was 0.4 nm, the fourth and fifth diffraction peak disappeared after annealing. At larger S_3N_4 layer thickness of 0.5 nm, only the fifth diffraction peak disappeared. It appears that a thick S_3N_4 layer is helpful to resist inter-diffusion at 900 °C and maintain the periodic layer structure.

Figures 8(a) and (b) are XRR patterns of CrN/Si_3N_4 coatings deposited at room temperature and after annealing at 900 °C for 4 h in which the S_3N_4 layer thickness is 0.3 nm and 0.8 nm, respectively. The CrN/Si_3N_4 multilayer with 0.3 nm thick Si_3N_4 also had apparent periodic layer structure after annealing at 900 °C for 4 h. The inter-diffusion between S_3N_4 and CrN was very poor due to the immiscibility and a very sharp interface was formed. There was no obvious change for XRR of the CrN/Si_3N_4 coatings with 0.8 nm thick Si_3N_4. Compared to the as-deposited sample, for the annealed sample a very weak, new higher order diffraction peak appeared. Perhaps this may be ascribed to the improvement of interface structure due to the thermodynamic driving effect. Hence, the thicker S_3N_4 layer was helpful for the thermal stability and stable periodic structure.

Figures 9(a) and (b) are XRD patterns of CrN/Si_3N_4 coatings deposited at room temperature and after annealing at 900 °C for 4 h with the S_3N_4 layer thickness of 0.3 and 0.8 nm. Even after annealing at 900 °C for 4 h, there is no evidence of Si_3N_4 diffraction peaks, which means that Si_3N_4 remains amorphous up to 900 °C. All CrN peaks become narrower after annealing. This indicates coarsening and/or reduced stress of the CrN grains. For CrN/Si_3N_4 coatings with a 0.8 nm thick S_3N_4 layer annealed at 900 °C, the (200) peak intensity becomes strong and the (111) peak intensity becomes weak.

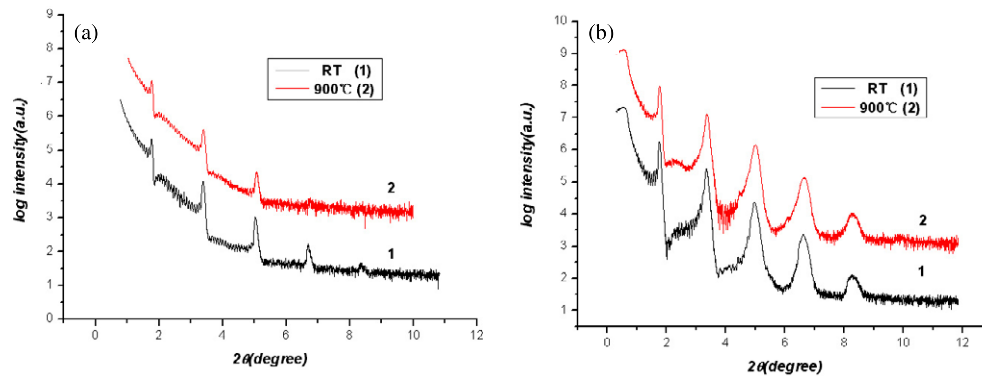

Figure 8. XRR patterns of CrN/Si_3N_4 coatings (20 layers) deposited at room temperature and after annealing at 900 °C for 4 h in which (a) CrN/Si_3N_4 layer thickness is 5.0/0.3 nm; (b) CrN/Si_3N_4 layer thickness is 5.0/0.8 nm.

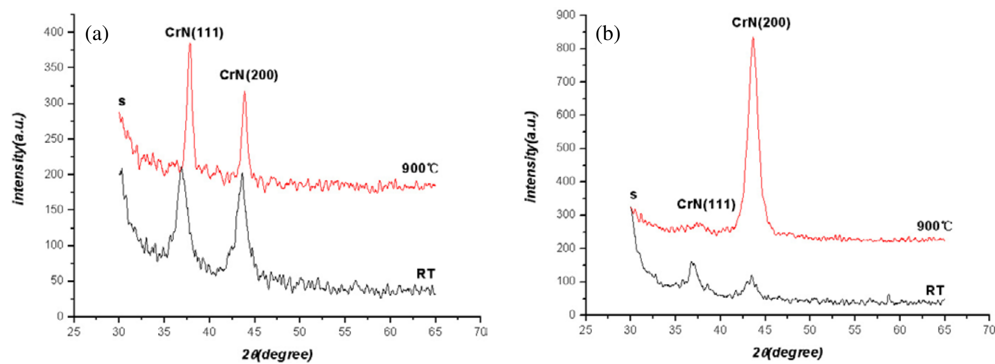

Figure 9. XRD patterns of CrN/Si_3N_4 coatings (20 layers) deposited at room temperature and after annealing at 900 °C for 4 h in which (a) CrN/Si_3N_4 layer thickness is 5.0/0.3 nm; (b) CrN/Si_3N_4 layer thickness is 5.0/0.8 nm.

4. Conclusions

This work demonstrates the effects of deposition parameters such as bias, pressure and substrate temperature on the interface structure and microstructure of CrN/Si_3N_4 multilayer coatings. The XRR spectra for CrN/Si_3N_4 multilayers with different thicknesses of Si_3N_4 show that the inter-diffusion between CrN and Si_3N_4 is very poor. The thermal stability of CrN/Si_3N_4 multilayer coatings depends on the Si_3N_4 layer thickness. At Si_3N_4 layer thickness of 0.8 nm, the layer structure of CrN/Si_3N_4 multilayer coatings is maintained very well after 4 h annealing at 900 °C. Even at Si_3N_4 layer thickness of 0.3 nm, the periodic layer structure is apparent. Therefore, the excellent thermal stability for the CrN/Si_3N_4 multilayer is significant for its applications in many fields [20].

Acknowledgments

The authors would like to thank Dr Beihong Long, Jun Zhang and Gang Peng for their help with the XRD and AFM measurements. The work was supported by the National

Science Foundation of China (grant No 50372024), the National Key Basic Research and Development Program (grant No 2004CB619301), and Project 985—Automotive Engineering of Jilin University.

References

[1] Derflinger V, Brandle H and Zimmermann H 1999 *Surf. Coat. Technol.* **113** 286
[2] Veprek S, Niederhofer A, Moto K, Bolom T, Mannling H-D, Nesladek P, Dollinger G and Bergmaier A 2000 *Surf. Coat. Technol.* **133/134** 152
[3] Veprek S, Haussmann M and Reiprich S 1996 *J. Vac. Sci. Technol.* A **14** 46
[4] Veprek S 1999 *J. Vac. Sci. Technol.* A **17** 2401
[5] Niederhofer A, Bolom T, Nesladek P, Moto K, Eggs C, Patil D S and Veprek S 2001 *Surf. Coat. Technol.* **146/147** 183
[6] Ma D, Ma S, Xu K and Veprek S 2005 *Mater. Lett.* **59** 838
[7] Veprek S, Haussmann M, Reiprich S, Li S and Dian J 1996 *Surf. Coat. Technol.* **86/87** 394
[8] Nose M, Chiou W A, Zhou M, Mae T and Meshii M 2002 *J. Vac. Sci. Technol.* A **20** 823
[9] Jagielski J, Khanna A S, Kucinski J, Mishra D S, Racolta P, Sioshansi P, Tobing E, Thereska J, Uglov V, Vilaithong T, Viviente J, Yang S-Z and Zalar A 2000 *Appl. Surf. Sci.* **156** 47
[10] Xu J, Hattori K, Seino Y and Kojima I 2002 *Thin Solid Films* **414** 239
[11] Martinez E, Sanjines R, Karimi A, Esteve J and Levy F 2004 *Surf. Coat. Technol.* **180/181** 570
[12] Chen Y-H, Guruz M, Chung Y-W and Keer L M 2002 *Surf. Coat. Technol.* **154** 162
[13] Veprek S, Veprek-Heijman Maritza G J, Karvankova P and Prochazka J 2005 *Thin Solid Films* **476** 1
[14] Ying G, Shao J and Fan Z 1993 *Chin. J. Lasers* **20** 900 (in Chinese)
[15] Wainfan N and Paratt L G 1960 *J. Appl. Phys.* **31** 1331
[16] Sarioglua C, Demirlerb U and Kursat Kazmanlib M 2005 *Surf. Coat. Technol.* **190** 238
[17] Lewis D B, Luo Q, Hovsepian P Eh and Munz W-D 2004 *Surf. Coat. Technol.* **184** 225
[18] Xu J, Yu L, Azuma Y, Fujimoto T, Umehara H and Kojima I 2002 *Appl. Phys. Lett.* **81** 4139
[19] Veprek S and Argon A S 2002 *J. Vac. Sci. Technol.* B **20** 650
[20] Yanga S, Wiemannb E and Teera D G 2004 *Surf. Coat. Technol.* **188/189** 662